

# A Quantum-Enhanced Prototype Gravitational-Wave Detector

K. Goda,<sup>1</sup> O. Miyakawa,<sup>2</sup> E. E. Mikhailov,<sup>3</sup> S. Saraf,<sup>4</sup> R. Adhikari,<sup>2</sup> K. McKenzie,<sup>5</sup> R. Ward,<sup>2</sup> S. Vass,<sup>2</sup> A. J. Weinstein,<sup>2</sup> and N. Mavalvala<sup>1</sup>

<sup>1</sup>*LIGO Laboratory, Massachusetts Institute of Technology, Cambridge, Massachusetts 02139 USA*

<sup>2</sup>*LIGO Laboratory, California Institute of Technology, Pasadena, California 91125 USA*

<sup>3</sup>*The College of William & Mary, Williamsburg, Virginia 23187 USA*

<sup>4</sup>*Rochester Institute of Technology, Rochester, New York 14623 USA*

<sup>5</sup>*Center for Gravitational Physics, The Australian National University, ACT 0200, Australia*

The quantum nature of the electromagnetic field imposes a fundamental limit on the sensitivity of optical precision measurements such as spectroscopy, microscopy, and interferometry [1]. The so-called quantum limit is set by the zero-point fluctuations of the electromagnetic field, which constrain the precision with which optical signals can be measured [2, 3, 4]. In the world of precision measurement, laser-interferometric gravitational wave (GW) detectors [4, 5, 7] are the most sensitive position meters ever operated, capable of measuring distance changes on the order of  $10^{-18}$  m RMS over kilometer separations caused by GWs from astronomical sources [8]. The sensitivity of currently operational and future GW detectors is limited by quantum optical noise [7]. Here we demonstrate a 44% improvement in displacement sensitivity of a prototype GW detector with suspended quasi-free mirrors at frequencies where the sensitivity is shot-noise-limited, by injection of a squeezed state of light [1, 2, 3]. This demonstration is a critical step toward implementation of squeezing-enhancement in large-scale GW detectors.

## I. INTRODUCTION

Laser-interferometric GW detectors, such as those of the Laser Interferometer Gravitational-Wave Observatory (LIGO) [5], are designed to measure distance changes on the order of  $10^{-18}$  m, or one-thousandth the diameter of the proton, caused by GWs from astronomical sources such as neutron star or black hole binaries, supernovae, and the Big Bang [8]. Their goals are to further verify Einstein's theory of general relativity and open an entirely new window onto the universe [5, 8]. The sensitivity of currently operational GW detectors is largely limited by quantum optical noise. Next-generation GW detectors, such as Advanced LIGO [7], planned to be operational in the next few years, are anticipated to be limited in sensitivity by quantum optical noise at almost all frequencies in the GW detection band (10 Hz – 10 kHz). The mirrors used in these interferometric GW detectors are suspended as pendulums, serving as quasi-free test masses in the GW detection band [5]. The quantum noise arises from uncertainty products associated with the commutation relations between conjugate field operators.

The quantum limit can be circumvented by use of nonclassical or *squeezed* states of light [1, 2, 3], where fluctuations are reduced below the symmetric quantum limit in one quadrature at the expense of increased fluctuations in the canonically conjugate quadrature. Squeezed states comprise a phase-dependent distribution of zero-point fluctuations such that the fluctuations in one quadrature are smaller than those of a coherent state, at the expense of increased fluctuations in the canonically conjugate quadrature, while preserving the Heisenberg limit on the uncertainty product. Since squeezed states were first observed by Slusher *et al.* in 1985 [9], a number of experimental efforts have realized the proof-of-principle of quantum noise reduction or squeezing-enhancement in various high-precision applications, such as spectroscopic measurement [10], lateral displacement measurement and imaging [11, 12], polarization measurement [13], and interferometric phase measurement [14]. Incorporating the technique of squeezing-enhancement into practical devices has remained a great challenge, either because the quantum limit is not reached due to excess classical noise, or because it is less onerous to enhance sensitivity by optimizing other parameters classically. Squeezed states are a useful ingredient for quantum teleportation [15], quantum cryptography [16], and quantum lithography [17], but these applications are yet to reach the stage of practical implementation, in part due to the complexity and technical challenges of working with squeezed states.

Laser-interferometric GW detectors such as LIGO [5], VIRGO [18], GEO600 [19], and TAMA300 [20] are so sensitive (they measure distance changes of  $10^{-18}$  m over kilometer separations) that they have already confronted the quantum limit [6]. In next-generation detectors, such as Advanced LIGO [7], optimization of classical parameters will reach the limits of technology. Any further improvement in sensitivity must rely on quantum techniques such as squeezing-enhancement, making GW detectors an important practical application of squeezed states of light.

The quantum nature of light reveals itself in two effects that limit the precision of an optical measurement of mirror position in laser-interferometric GW detectors: (i) *photon shot noise*, which typically dominates at frequencies above 100 Hz, arises from quantum uncertainty in the number of photons at the interferometer output; and (ii) *quantum radiation pressure noise*, typically dominant at frequencies below 100 Hz, that arises from mirror displacements

induced by quantum radiation pressure fluctuations [7, 21]. Both effects are caused by quantum fluctuations of a vacuum electromagnetic field that enters the antisymmetric port of the interferometer [4]. The displacement noise associated with the shot noise and quantum radiation pressure noise of a simple Michelson interferometer on a dark fringe in the frequency domain is given by [5]

$$\Delta x_{\text{shot}} = \sqrt{\frac{\hbar c \lambda}{\pi P}} \quad \text{and} \quad \Delta x_{\text{rad}} = \sqrt{\frac{\hbar P}{\pi^3 c \lambda m^2 f^4}}, \quad (1)$$

where  $c$  is the speed of light in vacuum,  $\hbar$  is Planck's constant,  $\lambda$  is the laser wavelength,  $m$  is the (reduced) mass of the mirrors,  $f$  is the measurement frequency, and  $P$  is the optical power incident on the beamsplitter.

The quantum limit in the laser-interferometric GW detector can be overcome by the injection of squeezed states of light into the antisymmetric port of the interferometer [4]. Following the 1981 proposal of Caves [4] to improve the sensitivity of quantum-noise-limited laser interferometers by squeezed state injection, a handful of experimental efforts have realized the proof-of-principle on the table-top scale at MHz frequencies [14, 22, 23]. Our demonstration of squeezing-enhancement shows improved sensitivity in a suspended-mirror prototype GW detector by injecting a squeezed vacuum field with an *inferred* level of  $9.3 \pm 0.1$  dB relative to shot noise into the antisymmetric port (see Methods). An important distinction between our experiment and previous efforts is that it is the first implementation of squeezing-enhancement in a prototype GW detector with suspended optics and a control and readout scheme similar to those used in the currently operational LIGO detectors, making it necessary to confront dynamical effects introduced by suspended mirrors such as optical springs [24]. It is, therefore, a critical step toward implementation of squeezing-enhancement in large-scale GW detectors. In all these experiments, including the one reported here, quantum radiation pressure noise was buried under other technical noise sources such as seismic noise and mirror thermal noise, and only the shot noise limit was accessible (not buried under technical noise) for showing squeezing-enhancement. As of today, quantum radiation pressure noise has not been observed in any experimental setting.

Terrestrial GW detectors typically comprise a Michelson interferometer with a Fabry-Perot cavity in each arm, to increase the phase sensitivity of the detector. The Michelson interferometer is operated on or near a dark fringe. Since most of the incident light returns toward the laser source, the GW-induced signal can be increased by recycling the laser power back toward the beamsplitter. This is achieved by placing a partially transmitting mirror – the “power recycling” mirror – between the laser source and the beamsplitter. Typical power recycling gains of 30 to 70 have been realized in presently operational GW detectors. Similarly, a partially transmissive mirror can also be placed at the antisymmetric port of the beamsplitter to further enhance the GW-induced signal at the interferometer output. This “signal recycling” mirror forms a complex optical cavity with the rest of the interferometer. The frequency-dependent optical response of the detector to incident GWs can be tuned by operating the signal recycling cavity at various detunings from resonance. Signal recycling is utilized in the GEO600 detector [19], and is planned for the Advanced LIGO detector [7].

## II. EXPERIMENT

The experiment reported here used a sub-configuration of the complete Advanced LIGO interferometer – a signal-recycled Michelson interferometer (SRMI), chosen in part because it is an important new feature of the optical configuration envisioned for Advanced LIGO [7, 24]. The shot noise limited displacement sensitivity of the SRMI is given in the frequency domain by [25]

$$\Delta x_{\text{SRMI}} = \frac{1}{\sqrt{|G|}} \sqrt{\frac{\hbar c \lambda}{\pi \eta P}} e^{-R}, \quad (2)$$

where  $G$  is the signal-recycling gain, given by  $G = [t_s / (1 - r_s r_m e^{-2i\phi})]^2$ ,  $\eta$  is the power transmission efficiency from the signal-recycling mirror to the photodetector (including the quantum efficiency of the photodetector), and  $R$  is the squeeze factor [3]. Here  $r_s$  and  $t_s$  are the amplitude reflectivity and transmissivity of the signal-recycling mirror,  $r_m$  is the reflectivity of the Michelson interferometer, and  $\phi$  is the signal-recycling cavity detuning. We note that setting  $G = 1$  and  $R = 0$  leads to the familiar expression for the shot noise limit in a Michelson interferometer, given in Eq. 1. In the experiment described below,  $\eta$ ,  $r_s$ , and  $r_m$  are measured to be 0.825,  $\sqrt{0.925}$ , and  $\sqrt{0.995}$  respectively, and  $P$  and  $\phi$  are obtained from fits to be 57 mW and 0, respectively.

This experiment was carried out in a prototype GW detector with suspended mirrors [24], designed to closely mimic the kilometer-scale LIGO detectors. A schematic of the experiment is shown in Fig. 1. Its major components are (i) an intensity- and frequency-stabilized Nd:YAG Master Oscillator Power Amplifier (MOPA) laser with a throughput of 5 W at 1064 nm that serves as the light source for both the interferometer and the squeezed vacuum generator; (ii)

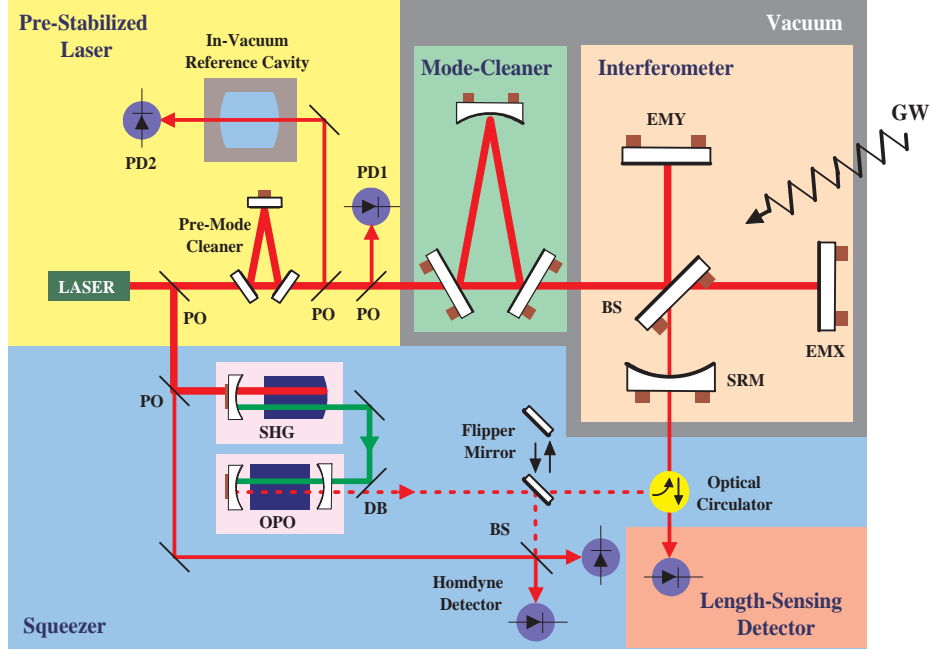


FIG. 1: Schematic of the quantum-enhanced prototype gravitational-wave (GW) detector that consists of five parts. BS: 50/50 beamsplitter; PD1 and PD2: photodetectors; PO: pickoff beamsplitter; DB: dichroic beamsplitter; SRM: signal-recycling mirror; EMX/EMY: end mirrors along the x/y axis, respectively; SHG: second-harmonic generator; OPO: optical parametric oscillator; GW: gravitational wave. The SHG, OPO, reference cavity, pre-mode cleaner, mode-cleaner, and signal-recycling cavity are all locked by adaptations of Pound-Drever-Hall locking [27]. PD1 and PD2 are used for the laser intensity and frequency stabilization while two photodetectors in the interferometer (not shown) and the length sensing detector are used to control the interferometer. All the mode-cleaner and interferometer optics are suspended by single loop pendulums.

a triangular optical cavity – or mode cleaner – which consists of three free hanging mirrors with a linewidth of 4 kHz to further stabilize the intensity, frequency, and mode of the laser; (iii) a test interferometer configured as a SRMI, comprising a 50/50 beamsplitter, two high-reflectivity end mirrors, and a signal-recycling mirror, all suspended as single loop pendulums (causing the optics to behave as inertial free masses); (iv) a squeezed vacuum generator – or squeezer – that consists of a second-harmonic generator (SHG), a sub-threshold vacuum-seeded optical parametric oscillator (OPO) pumped by a second-harmonic field, a monitor homodyne detector, and an optical circulator to inject the generated squeezed vacuum field to the interferometer; and (v) a high quantum efficiency photodetector to sense differential motion of the interferometer mirrors. The Michelson interferometer is locked on a dark fringe using a static differential offset such that a small amount of the carrier light exits the signal-recycling cavity, while the signal-recycling cavity is locked on a carrier resonance. This DC component of the carrier light at the antisymmetric port acts as a local oscillator field for a GW-induced signal to beat against, forming a homodyne detection or “DC readout” scheme [7].

The noise performance of the interferometer is shown in Fig. 2. The comparison between the measured noise floor without squeezing and the theoretically predicted noise floor based on the measured optical power of  $100 \mu\text{W}$  indicates that the interferometer is shot-noise-limited at frequencies above 42 kHz. In addition, the interferometer output power is changed by adjusting the Michelson offset to verify the  $\sqrt{P}$  scaling of the shot noise spectral density. At frequencies below 42 kHz, the noise is dominated by laser intensity noise and uncontrolled length fluctuations of the interferometer. The peaks at frequencies above 42 kHz are also due to the interferometer length fluctuations. In the shot-noise-limited frequency band, the detector sensitivity is  $(6.9 \pm 0.1) \times 10^{-17} \text{ m}/\sqrt{\text{Hz}}$ . Systematic uncertainty in the displacement calibration is estimated to be 10%, but does not affect the relative improvement achieved by squeeze injection that was observed.

### III. RESULTS

The result of the squeezing-enhancement in the interferometer is also shown in Fig. 2. The comparison between the two spectra shows that the noise floor of the interferometer was reduced by the injection of the squeezed vacuum field

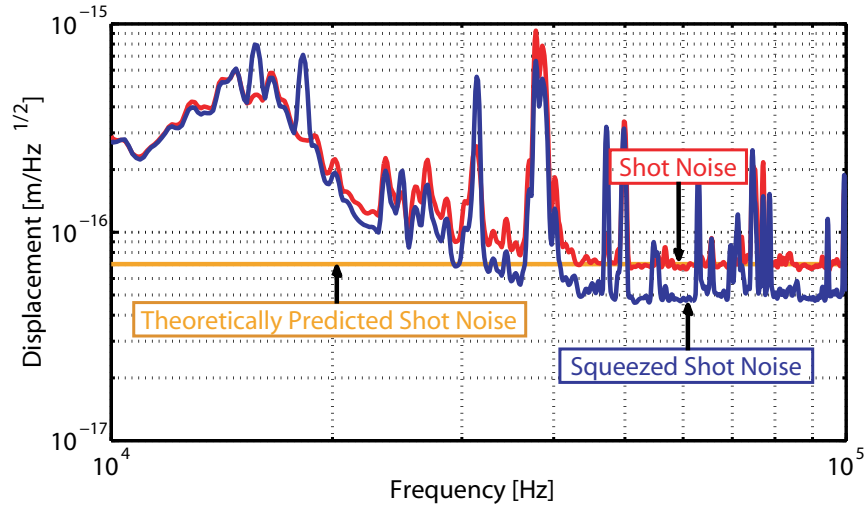


FIG. 2: The noise floor of the signal-recycled Michelson interferometer with (blue) and without (red) the injection of squeezed vacuum. The theoretically predicted shot noise level based on the measured optical power is also shown (orange). The interferometer is shot-noise-limited at frequencies above 42 kHz. Injection of squeezing leads to broadband reduction of the shot noise in the shot-noise-limited frequency band.

in the shot-noise-limited frequency band. Fig. 3 shows the noise floor with a simulated GW signal at 50 kHz, with and without injected squeezing. The broadband quantum noise floor was reduced from  $(6.9 \pm 0.1) \times 10^{-17} \text{ m}/\sqrt{\text{Hz}}$  to  $(4.8 \pm 0.1) \times 10^{-17} \text{ m}/\sqrt{\text{Hz}}$ , while the strength of the simulated GW signal was retained. This corresponds to a 44% increase in signal-to-noise ratio (SNR) or detector sensitivity. In kilometer-scale GW detectors, this would correspond to a factor of  $1.44^3 = 3.0$  increase in detection rate for isotropically distributed GW sources. The squeeze factor is found to be  $R = 0.36 \pm 0.03$  where the error comes from the variance in each noise floor. Other peaks in the squeezing spectrum are due to optical crosstalk between the interferometer and OPO, arising from inadequate isolation of the OPO from the interferometer output. It can be completely resolved by improved Faraday isolation, or use of an OPO in a bow-tie cavity configuration that geometrically separates the two fields [26], and is not expected to be a problem in operational GW detectors.

The measurable squeezing effect was limited to frequencies above 42 kHz in this experiment, since the quantum noise is masked by classical noise at lower frequencies. Many of the factors that led to this limit in the experiment presented here are not expected to effect squeezing-enhancement in the LIGO interferometers. One of the greatest challenges of using suspended mirrors – a crucial feature of this work – is the coupling of seismic noise to the detector output, due to large fluctuations in the positions and angles of the mirrors. In addition to the seismic noise coupling, laser frequency and intensity fluctuations also degrade the low frequency performance of the detector. Unlike the urban campus siting of the prototype detector used here, the LIGO detectors are located in remote sites with much quieter seismic and acoustic environments, and are equipped with better vibration isolation and mirror control systems. Moreover, in the kilometer-scale detectors, the long Fabry-Perot cavities act as optical filters to mitigate laser noise in the GW band [6]. Other challenges associated with suspended-mirror interferometry that had to be overcome in the present experiment include control of the mode overlap between the (relatively static) squeezed input and (dynamically fluctuating) interferometer output fields, interfacing of the in-vacuum parts of the experiment (the interferometer) with external optical systems (the squeezer), and optical isolation to mitigate optical feedback. Consequently, we expect the squeezing-enhancement to be effective at lower frequencies within the GW detection band when implemented on the long baseline LIGO detectors. This implementation of squeezing-enhancement in a GW detector prototype with the suspended optics and the readout and control scheme similar to those used in the currently operational LIGO detectors firmly establishes the practical feasibility of squeezing injection for future improvements to existing GW detectors worldwide.

#### IV. EXPERIMENTAL DETAILS

Each optic of the interferometer is suspended as a single loop pendulum mounted on a passive vibration isolation system within a single vacuum volume with a pressure of  $10^{-6}$  torr. At frequencies above the pendulum resonant

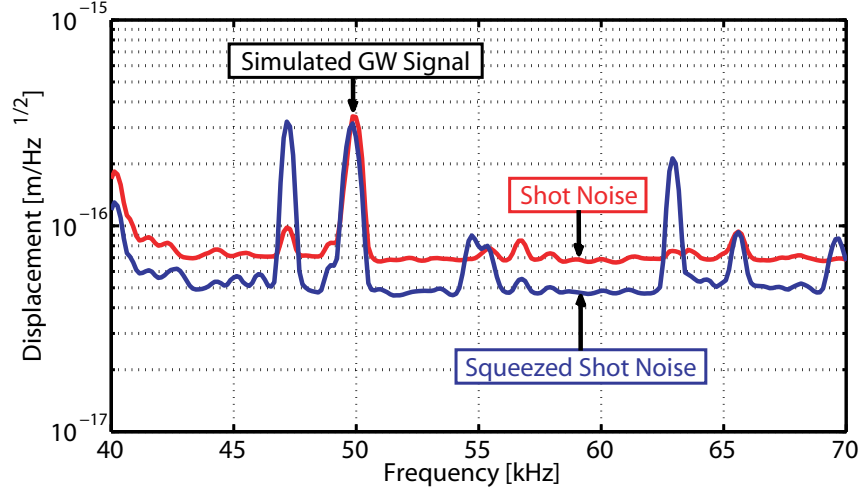


FIG. 3: A zoomed graph of the noise floor of the interferometer with a simulated gravitational-wave (GW) signal at 50 kHz with (blue) and without (red) the injection of squeezed vacuum. The simulated GW was generated by exciting the beamsplitter of the interferometer. The broadband shot noise floor was reduced from  $(6.9 \pm 0.1) \times 10^{-17} \text{ m}/\sqrt{\text{Hz}}$  to  $(4.8 \pm 0.1) \times 10^{-17} \text{ m}/\sqrt{\text{Hz}}$  by the injection of squeezing while the strength of the simulated GW signal was retained, resulting in a 44% increase in signal-to-noise ratio or detector sensitivity.

frequency ( $\sim 1 \text{ Hz}$ ), the suspensions attenuate seismic noise, causing the optics behave as inertial free masses. The mirrors are held in place by feedback control designed to suppress low-frequency seismically driven motion. Magnets affixed to each optic are surrounded by current-carrying coils that actuate on the mirror positions and angles. Adaptations of the Pound-Drever-Hall locking [27] are used to keep the mirrors of the interferometer at the desired operating point. More details can be found in Refs. [24, 28].

The OPO, operated below threshold, is used to produce a squeezed state by correlating the upper and lower quantum sidebands centered around the carrier frequency, in the presence of an energetic pump field. Since all GW detectors presently use high power Nd:YAG lasers sources at 1064 nm, generating squeezed states at 1064 nm is essential. The OPO is a cavity composed of a 10 mm long quasi-phase matched periodically-poled KTiOPO<sub>4</sub> crystal with anti-reflection coated flat surfaces and two external coupling mirrors [29]. To generate a low-frequency squeezed state, the OPO is vacuum-seeded and pumped by 320 mW of a second-harmonic field which is generated by the SHG from the same laser source that is incident on the interferometer. An auxiliary laser that is frequency-shifted by 642 MHz relative to the carrier frequency is used to lock the OPO cavity by using a PZT on one of the coupling mirrors. This frequency-shifted light is orthogonally polarized to the vacuum field that seeds the OPO cavity and to the pump field, and therefore, does not enter the interferometer. This type of OPO locking scheme is necessary to generate a squeezed state of *vacuum* which is squeezed at all frequencies, not a squeezed state of *light* which is typically squeezed only at MHz frequencies due to laser excess noise at frequencies below 1 MHz [23, 25].

The balanced homodyne detector is used to monitor the generated squeezed vacuum field before injection to the interferometer. It is composed of a 50/50 beamsplitter and a pair of photodiodes with matched quantum efficiencies of 93%. With a mode-cleaned coherent local oscillator field, the homodyne efficiency of this readout is 99.2%. The squeezing level measured by this detector is  $7.4 \pm 0.1 \text{ dB}$  [29]. Based on this value and the composite detection efficiency, the squeezing level at the output of the OPO is inferred to be  $9.3 \pm 0.1 \text{ dB}$  [25, 29].

The squeezed vacuum field is injected into the antisymmetric port of the interferometer via an optical circulator, a mode-matching telescope, and steering mirrors. To ensure a high coupling efficiency of the squeezed vacuum field to the interferometer field, the transmission of the interferometer output through the OPO cavity in a TEM<sub>00</sub> mode with the interferometer locked on a bright fringe is optimized by using the steering mirrors and mode-matching telescope. With the OPO cavity length scanned, the mode structure of the OPO transmission indicates the coupling efficiency of the interferometer mode to the OPO cavity mode or equivalently the optical loss due to the mode-mismatch between the interferometer and squeezed vacuum fields.

The interferometer output is detected by the length sensing photodetector with a quantum efficiency of 93%. To show the validity of squeezing, it is critical to calibrate the shot noise level correctly. Since the Michelson interferometer and signal-recycling cavity are locked by using RF sidebands (as well as the DC carrier light at the length sensing detector), it is important to verify that the carrier-to-sideband power ratio is sufficiently high so that the contribution of the sideband shot noise to the overall shot noise is small. Once the Michelson interferometer and signal-recycling



cavity are locked, the Michelson offset feedback control system is turned on and the offset is optimized such that the interferometer output power is  $100\ \mu\text{W}$ . It is also important to optimize the control gain to stabilize the power so that drift of the shot noise level is sufficiently lower than the effective squeezing level. The electronic noise of the readout is 6 dB below the shot noise. The combination of the detection efficiency (93%), the squeezing injection efficiency associated with the injection and round-trip loss (77.5%), the mode-overlap efficiency between the squeezed vacuum and interferometer field (96.0%), and the interferometer response determined by the reflectivity of the end test masses (99.5%), the reflectivity of the signal-recycling mirror (92.5%), and the Michelson offset ( $\pi/238$ ) attenuates the injected squeezing level of  $9.3\pm0.1$  dB down to about 3 dB [25].

The squeezing phase is locked to the amplitude quadrature of the interferometer field by the noise-locking technique [30] using a PZT-actuated mirror. It is critical to stably control the squeezing phase relative to the interferometer field since the anti-squeezing would, otherwise, degrade the shot noise level.

- 
- [1] Scully, M. O. & Zubairy, M. S. *Quantum Optics* (Cambridge University Press, Cambridge, 1997).
  - [2] Breitenbach, G., Schiller, S. & Mlynek, J. Measurement of the quantum states of squeezed light. *Nature* **387**, 471–475 (1997).
  - [3] Walls, D. F. Squeezed states of light. *Nature* **306**, 141–146 (1983).
  - [4] Caves, C. M. Quantum-mechanical noise in an interferometer. *Phys. Rev. D* **23**, 1693–1708 (1981).
  - [5] Abramovici, A. et al. LIGO: The Laser Interferometer Gravitational-Wave Observatory. *Science* **256**, 325–333 (1992).
  - [6] Abbott, B. et al. LIGO: The Laser Interferometer Gravitational-Wave Observatory. Submitted to *Rev. Mod. Phys.* (2007). Preprint/0711.3041.
  - [7] <http://www.ligo.caltech.edu/advLIGO> (2001).
  - [8] Thorne, K. S. In *300 Years of Gravitation* (Cambridge University Press, Cambridge, 1987).
  - [9] Slusher, R. E., Hollberg, L. W., Yurke, B., Mertz, J. C. & Valley, J. F. Observation of squeezed states generated by four-wave mixing in an optical cavity. *Phys. Rev. Lett.* **55**, 2409–2412 (1985).
  - [10] Polzik, E. S., Carri, J. & Kimble, H. J. Spectroscopy with squeezed light. *Phys. Rev. Lett.* **68**, 3020–3023. (1992).
  - [11] Treps, N. et al. Surpassing the standard quantum limit for optical imaging using nonclassical multimode light. *Phys. Rev. Lett.* **88**, 203601 (2002).
  - [12] Treps, N. et al. A quantum laser pointer. *Science* **301**, 940–943 (2003).
  - [13] Grangier, P., Slusher, R. E., Yurke, B. & LaPorta, A. Squeezed-light-enhanced polarization interferometer. *Phys. Rev. Lett.* (1987).
  - [14] Xiao, M., Wu, L.-A. & Kimble, H. J. Precision measurement beyond the shot-noise limit. *Phys. Rev. Lett.* **59**, 278–281 (1987).
  - [15] Furusawa, A. et al. Unconditional quantum teleportation. *Science* **282**, 706–709 (1998).
  - [16] Grosshans, F. & Grangier, P. Continuous variable quantum cryptography using coherent states. *Phys. Rev. Lett.* **88**, 057902 (2002).
  - [17] Boto, A. N. et al. Quantum interferometric optical lithography: Exploiting entanglement to beat the diffraction limit. *Phys. Rev. Lett.* **85**, 2733–2736 (2000).
  - [18] Fiore, L. D. & the VIRGO Collaboration. The present status of the VIRGO central interferometer. *Class. Quant. Grav.* **19**, 1421–1428 (2002).
  - [19] Willke, B. & the GEO Collaboration. The GEO600 gravitational wave detector. *Class. Quant. Grav.* **19**, 1377–1387 (2002).
  - [20] Ando, M. & the TAMA Collaboration. Stable operation of a 300-m laser interferometer with sufficient sensitivity to detect gravitational-wave events within our Galaxy. *Phys. Rev. Lett.* **86**, 3950–3954 (2001).
  - [21] Kimble, H. J., Levin, Y., Matsko, A. B., Thorne, K. S. & Vyatchanin, S. P. Conversion of conventional gravitational-wave interferometers into quantum nondemolition interferometers by modifying their input and/or output optics. *Phys. Rev. D* **65**, 022002 (2002).
  - [22] McKenzie, K., Shaddock, D. A., McClelland, D. E., Buchler, B. C. & Lam, P. K. Experimental demonstration of a squeezing-enhanced power-recycled Michelson interferometer for gravitational wave detection. *Phys. Rev. Lett.* **88**, 231102 (2002).
  - [23] Vahlbruch, H. et al. Demonstration of a squeezed-light-enhanced power- and signal-recycled Michelson interferometer. *Phys. Rev. Lett.* **95**, 211102 (2005).
  - [24] Miyakawa, O. et al. Measurement of optical response of a detuned resonant sideband extraction gravitational wave detector. *Phys. Rev. D* **74**, 022001 (2006).
  - [25] Goda, K. *Development of Techniques for Quantum-Enhanced Laser-Interferometric Gravitational-Wave Detectors* (Ph.D. Thesis, Massachusetts Institute of Technology, 2007).
  - [26] Grosse, N. B., Bowen, W. P., McKenzie, K. & Lam, P. K. Harmonic entanglement with second-order nonlinearity. *Phys. Rev. Lett.* **96**, 063601 (2006).
  - [27] Drever, R. W. P. et al. Laser phase and frequency stabilization using an optical resonator. *Appl. Phys. B* **31**, 97–105 (1983).
  - [28] Abbott, B. et al. Conceptual design of the 40 meter laboratory upgrade for prototyping a Advanced LIGO interferometer.

- LIGO Technical Note, LIGO-T010115-R (2001).
- [29] Goda, K. et al. Generation of a stable low-frequency squeezed vacuum field with periodically poled KTiOPO<sub>4</sub> at 1064 nm. Opt. Lett. **33**, 92-94 (2008).
- [30] McKenzie, K. et al. Quantum noise locking. J. Opt. B: Quantum Semiclass. Opt. **7**, S421–S428 (2005).